
How Incomplete is Contrastive Learning? An Inter-intra Variant Dual Representation Method for Self-supervised Video Recognition

Lin Zhang
Carnegie Mellon University
linz2@andrew.cmu.edu

Qi She
ByteDance AI Lab
sheqi1991@gmail.com

Zhengyang Shen
Peking University
1701110045@pku.edu.cn

Changhu Wang
ByteDance AI Lab
wangchanghu@bytedance.com

Abstract

Contrastive learning applied to self-supervised representation learning has seen a resurgence in deep models. In this paper, we find that existing contrastive learning based solutions for self-supervised video recognition focus on inter-variance encoding but ignore the intra-variance existing in clips within the same video. We thus propose to learn dual representations for each clip which (i) encode intra-variance through a shuffle-rank pretext task; (ii) encode inter-variance through a temporal coherent contrastive loss. Experiment results show that our method plays an essential role in balancing inter and intra variances and brings consistent performance gains on multiple backbones and contrastive learning frameworks. Integrated with SimCLR and pretrained on Kinetics-400, our method achieves **82.0%** and **51.2%** downstream classification accuracy on UCF101 and HMDB51 test sets respectively and **46.1%** video retrieval accuracy on UCF101, outperforming both pretext-task based and contrastive learning based counterparts.

1 Introduction

Labeled data is the fundamental resource in deep learning era however is laborious to acquire. To tackle this dilemma, researchers resort to self-supervised learning to learn from unlabeled data. Recent rapid development of self-supervised learning [3, 4, 8, 10] has been largely benefited from instance discrimination based contrastive learning [36]. With an InfoNCE loss [31], contrastive learning tries to pull examples sampled from the same instance (positive pairs) close to each other while repelling those from different instances (negative pairs). This loss is favored in image classification as augmentations of the same image does not change image semantics. As a result, recent works tried to transplant the same method into video representation learning [6, 22, 28], i.e. making clips sampled from the same video attracting each other. Though having achieved remarkable performances, we challenge that such learning goal does not conform to the innate inter-intra variance of videos which is the essential difference between *images* and *videos*, thus is incomplete for video representation learning. Specifically, video semantics rely on not only image-level appearances, but also the temporal variance, i.e. different clips sampled from different time spans of a video exhibit different semantics meanings. For instance, *running* and *jumping* are two different mini-actions though they are both sampled from a video classified as *HighJump*. Previous works [7, 16, 20, 35, 38] have proposed to learn such temporal differences using frame/clip order verification tasks. However, the order of sub-clips is largely determined by continuity instead of semantic difference between sub-clips.

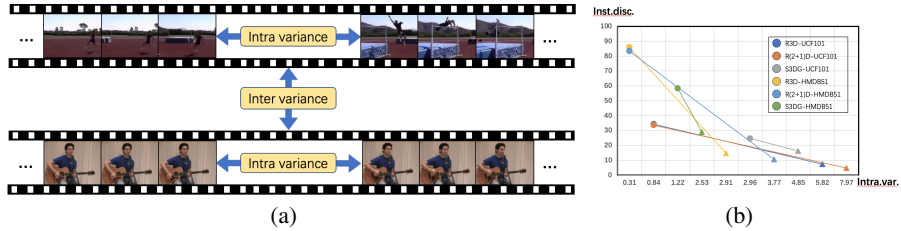


Figure 1: (a) Demonstration of inter and intra variances in videos. Contrastive learning only encodes inter-variance between different videos but ignores temporal intra-variance. We propose to jointly encode both inter and intra variances into dual representations for sub-clips. As intra-variance can be really subtle (bottom video) where classification becomes ambiguous, we adopt ranking loss to induce a small margin. (b) Instance discrimination factor and intra-variance value on feature computed on different pretrained backbones and datasets. Triangles mark our method while circles refers to SimCLR contrastive learning baseline. Our method consistently improves intra-variance while decreasing instance discrimination power. More details can be seen in Table 2.

Besides, some repetitive actions such as playing guitar seldom have changes between its sub-clips, in which case predicting order becomes ambiguous (Fig 1).

In this work, we delve into self-supervised video representation learning from the perspective of inter-intra variance encoding. We argue that a good self-supervised pretrained encoder should learn both inter and intra variances. Based on such motivation, we theoretically and experimentally show that contrastive learning [31] overemphasizes the learning of inter-variance but ignores intra-variance (Fig 1). Previous works [21, 33] tried to incorporate learning of intra-variance by appending an extra projection head for solely solving the pretext task. The two projection heads, contrastive head and pretext head, thus separately encode inter and intra variances. In contrast, our method learns dual representations for each clip, which not only encodes intra-variance between sub-clips by a shuffle-rank pretext task but also encodes inter-variance between different videos by a temporal coherent contrastive loss. Besides, we realize that intra-variance can be subtle depending on different videos and a large-margin-induced classification loss will spoil inter-variance encoding. Therefore, we adopt a ranking loss to induce a small margin between sub-clip features. We verify the effectiveness of our method by conducting a series of experiments on UCF101 [25] and HMDB51 [15] action recognition datasets. Results show that our method can indeed balance inter-intra feature variances (Fig 1) and consistently achieve performance gains. Moreover, our method also achieves superior performances on both finetuning downstream task and video retrieval task to state-of-the-arts. The proposed method can be applied to both SimCLR [4] and MoCo [10] contrastive learning frameworks and plugged into multiple spatial-temporal backbones for improvement.

In a nutshell, our contributions are 4-fold (i) We propose a shuffle-rank pretext task, which induces a small margin between intra-variant features, alleviating contradiction between inter-video and intra-video discrimination. (ii) We propose temporal coherent contrast on the dual representations to model inter variance learning. (iii) By enforcing shuffle-rank loss and temporal coherent contrast on dual representations, we learn a joint inter-intra variant representation as opposed to solely inter-variant representation in contrastive learning. We also conduct a series of experiments to validate the effectiveness of our method on inter-intra variance encoding. (iv) The proposed method can be flexibly applied to contractive learning frameworks, e.g., MoCo and SimCLR with multiple spatial-temporal backbones and achieves superior performances to state-of-the-art methods.

2 Related work

2.1 Self-supervised video recognition

We classify existing self-supervised video recognition methods into two categories based on type of the supervision signal enforced: pretext task based and contrastive learning based.

Pretext task based Pretext task based solutions design handcrafted tasks to solve. Verifying frame and clip order [7, 16, 20, 35, 38] can provide useful order information for downstream transferring. For example, Misra et al. [20] verified whether a tuple of frames were in the correct order or not. Xu et al. [38] chose verifying clip order instead of frame order as clip is more informative. Though effective, temporal order is largely based on smoothness of frame/clip changes thus cannot learn general clip variances. Besides, utilizing both spatial and temporal information [12, 19, 32] has also achieved remarkable performance. Wang et al. [32] proposed to learn spatial-temporal features by designing multiple spatial-temporal statistics prediction tasks. Relying on multiple sophisticated tasks, it has limited applications. Recently, exploring speedness in videos have become very popular [21, 23, 24, 33, 39]. Peihao et al. [21] found out that predicting relative speed instead of video-agnostic speedness exhibits better performance. In this paper, we also propose a simple pretext task named shuffle-rank which encodes temporal intra-variance between clips. The essential differences between our task and shuffling order prediction are (i) We aim to learn a variety of intra-variance between clips by comparing sub-clip feature similarities instead of simply predicting clip order, which is ambiguous when clip changes are small (Fig 1); (ii) Order classification loss induces a large margin between intra-variant sub-clip features, thus can spoil inter-variance encoding which requires features from the same video to be close. In contrast, our ranking loss induces a small margin, alleviating such potential contradiction between inter and intra variance encoding. We provide more discussions in section 4.2 and section 5.3.

Contrastive learning based Based on instance discrimination, contrastive learning tries to distinguish same instance from different ones. MoCo [10] designed a negative queue to retrieve more negative pairs. SimCLR [4] proved that simple batchwise instance discrimination can achieve superior performance by increasing the batch size. On video level, based on MoCo, Tian et al. [28] built a temporarily decayed negative queue to model temporal variance. Rui et al. [22] conducted sufficient experiments to study video-level SimCLR’s performance. Kong et al. [14] learned feature proximity between video and frame features. In [6], the author systematically analyzed four self-supervised learning frameworks on videos. However, all these contrastive learning methods aim to learn inter-video variance and intra-video invariance. Differently, Tao et al. [26] proposed an inter-intra contrastive learning framework by creating different positive and negative pairs. But they still encoded the whole clip without analyzing the sub-clip interactions, achieving little performance gains. In contrast, our work makes use of dual features to encode temporal differences between sub-clips and jointly utilized pretext tasks to achieve much better performance.

2.2 Intra-class and inter-class variance

Balancing inter-class variance and intra-class variance has been a critical research direction in various areas. Bai et al. [1] leveraged intra-class variance in metric learning to improve the performance of fine-grained image recognition. In few-shot image classification area, Liu et al. [17] found out that negative margins in softmax loss results in lower intra-class variance and higher inter-class variance for novel classes. To alleviate long-tailed distribution, Liu et al. [18] proposed to increase intra-variance of tail classes by augmenting it with feature distributions of head classes. In this paper, we instead treat each video as an individual class and study the effect of instance-wise intra and inter variances because data is unlabeled in self-supervised learning stage. In order to balance the inter-intra variance learning, we propose to learn sub-clip dual representations. We experimentally study the effect of our model on inter-intra variance learning in section 5.3.

3 Preliminary

In this section, we first introduce our understanding to inter-intra variances in video data, and then explain the disadvantage of contrastive learning in video data which only encodes inter-variance. This leads to our motivation of learning inter-intra variant dual representations in section 4.

3.1 Video data distribution with inter-intra variances

Suppose we have a collection of N unlabeled videos $\{V_i\}_{i=1}^N$. In video representation learning, due to the memory limit, we sample a total of M clips $\{c_i\}_{i=1}^M$ from videos, with $\frac{M}{N}$ clips per video. During self-supervised pretraining, a clip c_i is selected from a video and encoded by our model f into

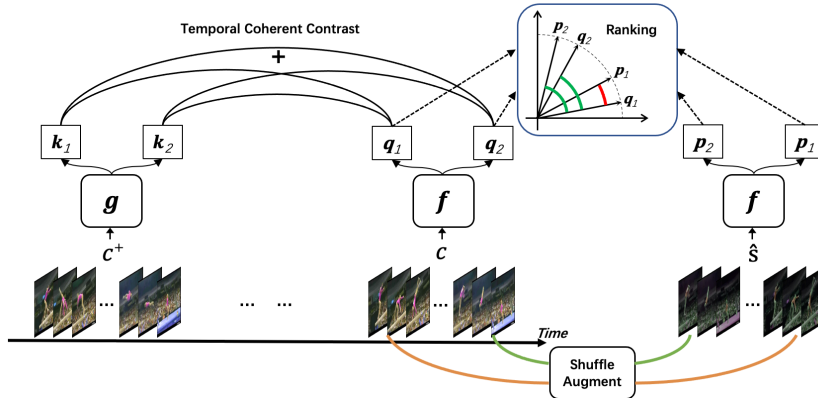


Figure 2: Method Overview. During the intra-variance learning stage, we shuffle and augment clip c into \hat{s} and encode it into dual representations p_1 and p_2 , which correspond to the unshuffled dual representations q_1 and q_2 respectively. If we treat q_1 as anchor, then representation of the same sub-clip (Red) should be ranked higher than that of different sub-clips (Green). During the inter-variance learning stage(left-hand side), the temporarily variant dual representations should however keep coherence in that all dual representations of clips sampled from the same video (c, c^+) should be regarded as positive pairs(+) in contrastive learning. Encoder g is momentum updated by f in MoCo but equals to f in SimCLR.

a normalized feature vector z_i , i.e. $z_i = f(c_i)$. The goal of self-supervised pretraining is to learn a good encoder f that can be well transferred to downstream task, e.g. video action recognition. For such a purpose, on one hand, the trained encoder should distinguish different videos since different videos have different contents and semantic meanings. This is known as inter-variance (σ_{inter}). On the other hand, though clips in the same video have similar contents, the mini-actions they represent can be completely different, e.g. *running* and *jumping* are two different mini-actions at different time spans of a video classified as *HighJump*. Our motivation is that, if an encoder can learn on both clip-level (*HighJump*) and sub-clip-level (*running* and *jumping*), it will have a more generalized transfer ability in the downstream tasks. We thus aim to produce embedded features $\{z\}$ that are both inter-variant and intra-variant.

3.2 Self-supervised contrastive representation learning

Typical self-supervised contrastive learning is based on instance discrimination, i.e. clips from the same video are expected to attract each other while repelling those from different videos. Formally, the contrastive loss is denoted as :

$$L_c = -\frac{1}{M} \sum_{i=1}^M \log \frac{\exp(z_i \cdot z_{i+} / \tau)}{\sum_{k=1}^M \mathbf{1}_{[k \neq i]} \exp(z_i \cdot z_k / \tau)} \quad (1)$$

where z_{i+} is a clip feature sampled from the same video of z_i , denoted as positive pair (+), and τ is a temperature parameter. We denote this typical contrastive learning as clip contrast since it only compares clip-level representations. We can easily extend the analysis in [29] to find that such contrastive learning has an objective of persistently increasing σ_{inter} and decreasing σ_{intra} , leading to an over-strong instance discrimination ability and insignificant intra-variance (see supplementary material). In this work, we aim to jointly learn σ_{intra} and σ_{inter} . To do so, we propose a shuffle-rank pretext task to compensate for lack of intra-variance in contrastive learning, then encode σ_{inter} by temporal coherent contrast between sub-clip dual representations.

4 Methodology

4.1 Dual representations

In contrastive learning, an n -frame clip is typically encoded globally into a single feature for similarity comparison. However, contrast between the inner sub-clips is not fully utilized. We instead use dual

feature vectors for representation, where each feature corresponds to half of the input clip (as seen in Fig 2).

Formally, in addition to the original clip projector, we add another projection head, denoted as dual projection head, after the backbone. Through dual projection head, a sampled clip c is projected into dual features $r = (q_1, q_2)$. Our goal is then to jointly encode the intra-variance and inter-variance into r , i.e. differences between two sub-clips of c and between c and other videos.

4.2 Shuffle-rank

To accurately encode the difference between two sub-clips into dual representations, raw sub-clips and learned dual features should be well aligned. We therefore apply a shuffle-rank pretext task. In this section, we first describe our method, then explain the differences between our method and order prediction, which has been extensively studied before [12, 20, 38].

Sub-clip shuffling Firstly, we uniformly divide clip c into two sub-clips c_1 and c_2 . In practice, c consists of 16 frames while c_1 and c_2 each consists of 8 frames. By apply data augmentation on $c = (c_1, c_2)$, we transform c into a new augmented clip $\hat{c} = (\hat{c}_1, \hat{c}_2)$, where *hat* refers to augmentation. We further shuffle \hat{c} to get its shuffled version $\hat{s} = (\hat{c}_2, \hat{c}_1)$. The shuffled and augmented clip \hat{s} is then projected into dual representations $\hat{r}^s = (p_2, p_1)$ through the dual projection head.

Representation ranking Our goal is to encode temporal intra-variance between sub-clips by enforcing the sub-clip feature correspondence, i.e. $\{c_1, \hat{c}_1\} \Leftrightarrow \{q_1, p_1\}$ and $\{c_2, \hat{c}_2\} \Leftrightarrow \{q_2, p_2\}$. We apply a ranking measure [2, 5] to learn this subtle intra-variance. Formally, if we regard q_1 as anchor, then p_1 should be ranked before both q_2 and p_2 . As the ranking between q_2 and p_2 is unknown, we adopt pairwise ranking, as shown in Fig 2. Penalties should be heavily imposed when such ranking is wrong and stay zero when the ranking is correct. However, directly applying such discrete loss would harm the stability of training. In order to have a smoother gradient backpropagation, we adopt the logistic loss function [2]. For a sub feature x , we denote its leave-self-out set of dual representations set as x^+ and its unpaired representations set as x^- , e.g. $q_1^+ = \{q_1, p_1\} \setminus \{q_1\} = \{p_1\}$, $p_1^+ = \{q_1, p_1\} \setminus \{p_1\} = \{q_1\}$, $q_1^- = \{q_2, p_2\}$ and $p_1^- = \{p_2, q_2\}$. Let S be a function mapping two clips to their dual features set, e.g. $S(c_i, \hat{s}_i) = \{q_1^i, q_2^i, p_1^i, p_2^i\}$, then the ranking loss between *unaugmented* original clips $\{c\}$ and their shuffled and augmented clips $\{\hat{s}\}$ is written as :

$$\mathcal{L}_{rank}^{unaug} = \sum_{i=1}^M \sum_{x \in S(c_i, \hat{s}_i)} \sum_{y \in x^+, z \in x^-} \log(1 + \exp(\frac{\text{sim}(x, z) - \text{sim}(x, y)}{\theta})) \quad (2)$$

where θ is a temperature parameter. In practice, for augmentation, we also compute ranking loss between *augmented* clips $\{s\}$ and $\{\hat{s}\}$, denoted as \mathcal{L}_{rank}^{aug} . Final ranking loss \mathcal{L}_{rank} is average of the two. In Fig 2, we only demonstrate the computing of $\mathcal{L}_{rank}^{unaug}$ for simplicity.

The adopted ranking loss is advantageous over order prediction in two aspects: (i) Order is only a subset of intra-video variance, whereas in our case, by comparing the pairwise similarities between sub-clip representations, a larger variety of intra-variance can be encoded. (ii) Softmax cross entropy loss based order prediction induces large margin between intra-video features [13], thus decreases the margin between inter-video features and is detrimental to inter-variance encoding. Instead, ranking loss only requires a small margin between similarity of positive intra pairs (x and x^+) and similarity of negative intra pairs (x and x^-). Such a loss is also safer since sub-clip differences vary a lot from video to video. For example, in a *Typing* video the scene seldom changes, exhibiting smaller intra-variance, while in a *ClipDiving* video both human action and the background scene change very fast, resulting in large intra-variance.

In section 5.3, we compare our shuffle-rank task with a common order prediction task. We also show that the temperature θ plays an important role in modeling such ranking effect and brings obvious improvement when θ is small enough.

4.3 Temporal coherent contrastive learning

We want to further encode the inter-variance into the dual features. To do so, coherence between dual features should be maintained in that dual features from clips in the same video should be closer to

each other in feature space than those from different videos, since inter-variance is much larger than intra-variance. We thus extend clip contrast to temporal coherent contrast by using sub-clip similarity instead of clip similarity. In particular, we denote similarity between two dual representations \mathbf{r}_i and \mathbf{r}_j as $\text{tc-sim}(\mathbf{r}_i, \mathbf{r}_j) = \frac{1}{4} \sum_{\mathbf{x} \in \mathbf{r}_i, \mathbf{y} \in \mathbf{r}_j} \mathbf{x} \cdot \mathbf{y}$ where \mathbf{r}_i and \mathbf{r}_j correspond to clips c_i and c_j respectively. Then the temporal coherent contrastive loss is written as:

$$\mathcal{L}_{tc} = -\frac{1}{M} \sum_{i=1}^M \log \frac{\exp(\text{tc-sim}(\mathbf{r}_i, \mathbf{r}_{i^+})/\tau_{tc})}{\sum_{k=1}^M \mathbf{1}_{[k \neq i]} \exp(\text{tc-sim}(\mathbf{r}_i, \mathbf{r}_k)/\tau_{tc})} \quad (3)$$

where τ_{tc} is a temperature parameter and i^+ indexes the i -th clip’s positive pair. Though simple, the temporal coherent contrastive learning further increases the inter-instance variances and instance discrimination ability of self-supervised learned models, and consistently improves the performance upon intra-variance encoded representations, as Table 1 shows.

Our final loss is the sum of clip contrastive loss, ranking loss and temporal coherent contrastive loss $\mathcal{L} = \mathcal{L}_c + \lambda_1 * \mathcal{L}_{rank} + \lambda_2 * \mathcal{L}_{tc}$, where λ_1 and λ_2 are hyperparameters.

5 Experiments

We conduct experiments on two contrastive learning frameworks (MoCo [10], SimCLR [4]) and three backbones (R3D [30], R(2+1)D [30], S3D-G [37]). We apply our method in pretraining stage and evaluate performance on two downstream tasks: finetuning the model and video retrieval.

5.1 Datasets

Kinetics400 Kinetics400 [11] is a large-scale video action dataset with 400 classes and more than 400 different videos for each class, licensed under CC-BY 4.0. All the videos are partial clips from Youtube and have a duration of around 10 seconds with varied resolutions. Original Kinetics400 has 240k training videos, but we are only able to obtain 218,846 videos due to invalid links.

UCF101 UCF101 [25] is a medium-scale human action video dataset with 13,320 videos classified into 101 classes. All the videos have a fixed frame rate of 25 FPS and a resolution of 320×240 . It provides 3 train-test splits. We use split 1 in all our experiments.

HMDB51 HMDB51 [15] is also a medium-scale human action video dataset with 6849 videos with 51 classes. The dataset is licensed under CC-BY 3.0. The videos are scaled to a height of 240 pixels and 30 FPS. Similarly, we use its split 1 for training and testing.

5.2 Implementations

Self-supervised pretrain In self-supervised pretraining stage, we randomly resize and crop images to size of 112×112 in a temporal consistent way. Each input clip has 16 frames with temporal interval of 4. Data augmentations include random color jittering, horizontal flipping and gaussian blurring. We pretrain the model for 200 epochs with an SGD optimizer with an initial learning rate of 0.003 and batch size of 64 on 8 Tesla V100 GPUs. Size of the MoCo negative queue is set to 16,384. We pretrain on UCF101 training split in all ablation studies and provide pretraining result on large-scale Kinetics400 for performance comparison with previous works. We set $\tau, \tau_{tc}, \theta, \lambda_1, \lambda_2$ to 0.07, 0.5, 0.05, 1.0 and 1.0, respectively.

Supervised finetuning During supervised finetuning, we replace the nonlinear projection head in pretraining stage with a one-layer classification layer. The backbone is initialized with the pretrained weights while the classification head is randomly initialized. We finetune all layers for 150 epochs on UCF101 and HMDB51 training splits with a batchsize of 64 and learning rate of 0.05. One input clip consists of 16 112×112 images sampled with temporal interval 2. After finetuning, we test classification accuracy on the test splits.

Video retrieval To evaluate the representation ability of pretrained model in a straightforward way, we use videos in test set to retrieve videos in training set. Specifically, we compute average features

Table 1: Experiments on MoCo and SimCLR with R3D, R(2+1)D and S3D-G backbones. Models are pretrained on UCF101 train split 1. SR refers to shuffle and rank pretext task. TC refers to temporal coherent contrastive learning. Improvement upon baseline is marked as **Red** superscripts.

	R3D		R(2+1)D		S3D-G	
	UCF101	HMDB51	UCF101	HMDB51	UCF101	HMDB51
MoCo	71.72	41.04	77.64	45.70	68.41	38.08
MoCo+SR	74.28 ^{+2.56}	44.06 ^{+3.02}	78.67 ^{+1.03}	46.09 ^{+0.39}	70.79 ^{+2.38}	40.12 ^{+2.04}
MoCo+SR+TC	74.65 ^{+2.93}	44.45 ^{+3.41}	78.46 ^{+0.82}	47.47 ^{+1.77}	72.19 ^{+3.78}	41.56 ^{+3.48}
SimCLR	71.90	39.79	71.61	31.78	66.27	20.16
SimCLR+SR	72.24 ^{+0.34}	40.38 ^{+0.59}	76.82 ^{+5.21}	40.05 ^{+8.27}	70.82 ^{+4.55}	34.73 ^{+14.57}
SimCLR+SR+TC	72.69 ^{+0.79}	43.01 ^{+3.32}	79.01 ^{+7.40}	45.37 ^{+13.59}	71.32 ^{+5.05}	35.33 ^{+15.17}

of 10 clips uniformly sampled from each video using the pretrained backbone. Features are computed through spatial-temporal average pooling the last layer output of the backbone. We conduct video retrieval on UCF101 and calculate the top- k accuracy ($k = 1, 5, 10, 20, 50$).

5.3 Ablation study

Effectiveness of proposed method We first show the effectiveness of our method by conducting experiments on both MoCo and SimCLR frameworks and three spatio-temporal backbones R3D, R(2+1)D and S3D-G. As Table 1 shows, consistent performance gains on multiple backbones can be observed. On SimCLR with R(2+1)D, equipping baseline with shuffle-rank and temporal coherent contrast can each increase accuracy on HMDB51 by 5.21% and 8.27%, and the integrated method can further increase accuracy to 7.40% and 13.59% respectively. It can be observed that performance improvements differ on different backbones and architectures, which might be due to (i) the internal structure of architecture (ii) baseline performance, e.g. a strong baseline performance means smaller space for improvement so the performance gain is smaller. However, even on a pretty strong baseline such as MoCo with R(2+1)D backbone, our integrated method can still improve accuracy on UCF and HMDB by 0.82% and 1.77% respectively.

Effect on inter and intra variance encoding To analyze the effect of our method on variance encoding, we explicitly calculate inter-intra variance of video features produced by pretrained backbone on UCF101 and HMDB51 test set. Specifically, we uniformly sample 10 clips for each video temporarily, then calculate σ_{inter} , σ_{intra} and instance discrimination factor $\sigma_{inter}/\sigma_{intra}$. The calculation formulas are defined in supplementary material. Intuitively, σ_{intra} refers to average variance of the 10 clip features for all videos and σ_{inter} refers to average pairwise variance between the mean features of different videos.

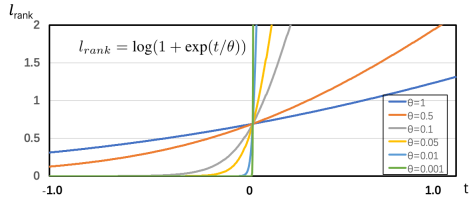
As shown in Table 2, shuffle-rank can always increase σ_{inter} by a large margin, e.g. 14 times on R(2+1)D on UCF101 from 0.0084 to 0.1123. After further adding temporal coherent contrast, σ_{inter} is increased to 0.0797 and σ_{intra} is decreased to 0.3798. Our method balances the instance discrimination ability from an overly strong level 33.60 to a medium value 4.77. This general phenomenon on all three backbones (R3D, R(2+1)D, S3D-G) and two datasets (UCF101, HMDB51) verifies our motivation, i.e. using shuffle-rank to encode intra-variance and temporal coherent contrast to further strengthen inter-variance encoding. It also supports our statement in section 3 that encoding intra-variance can be beneficial for self-supervised representation learning.

Comparison to shuffling order prediction Following our discussion in Section 4.2, we compare shuffle-rank to a non-trivial shuffling order prediction baseline. Our method is more friendly in encoding both inter and intra variances by using ranking loss. Our finetuning accuracy improves upon order prediction baseline from 75.39% and 32.38% to 76.82% to 40.05% on UCF101 and HMDB51 respectively. We report the table in the supplementary material.

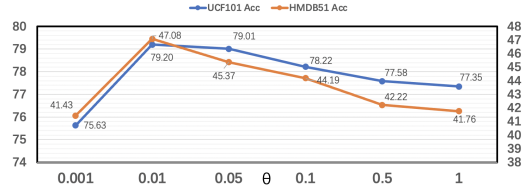
Effect of ranking loss parameter θ Following our discussion in Section 4.2, we validate our theoretical statement that inducing a smaller margin between intra positive and negative pairs brings larger benefits in jointly encoding inter and intra variance in Figure 3. In Figure 3 (a), we plot

Table 2: Comparison of inter-instance variance, intra-instance variance and instance discrimination factor. Results are multiplied by 100 for demonstration. Each cell’s increasing(Red) and decreasing(Green) times are compared to the cell above it.

	R3D			R(2+1)D			S3D-G		
	inter-v.	intra-v.	discrim.	inter-v.	intra-v.	discrim.	inter-v.	intra-v.	discrim.
UCF101									
SimCLR	28.83	0.84	34.3	28.22	0.84	33.6	73.13	2.96	24.7
+SR	22.64	11.30 ^{↑13.6×}	2.0 ^{↓17.2×}	23.00	11.23 ^{↑13.4×}	2.0 ^{↓16.8×}	51.71	11.73 ^{↑4.0×}	4.4 ^{↓5.6×}
+SR+TC	42.33	5.82 ^{↓1.9×}	7.3 ^{↑3.7×}	37.98	7.97 ^{↓1.4×}	4.8 ^{↑2.4×}	78.69	4.85 ^{↓2.4×}	16.2 ^{↑3.7×}
HMDB51									
SimCLR	26.60	0.31	85.8	25.82	0.31	83.3	71.14	1.22	58.3
+SR	33.72	5.81 ^{↑18.7×}	5.8 ^{↓14.8×}	32.24	5.07 ^{↑16.4×}	6.4 ^{↓13.0×}	61.84	4.81 ^{↑3.9×}	12.9 ^{↓4.5×}
+SR+TC	42.98	2.91 ^{↓2.0×}	14.8 ^{↑2.6×}	39.95	3.77 ^{↓1.3×}	10.6 ^{↑1.7×}	73.33	2.53 ^{↓1.9×}	29.0 ^{↑2.2×}



(a) Graph of ranking loss. t is the difference between negative and positive sub-clip pairs, i.e. $t = \text{sim}(\mathbf{x}, \mathbf{x}^-) - \text{sim}(\mathbf{x}, \mathbf{x}^+)$



(b) Finetuning accuracies on UCF101 and HMDB51 test set.

Figure 3: Under different θ values, we (a) plot ranking loss graph (b) investigate effect of θ on downstream classification accuracy. Decreasing θ induces a smaller margin ($|t|$) under the same l_{rank} and improves finetuning performance.

ranking loss (l_{rank}) graph under different θ settings. When the difference between similarities of intra negative and positive pairs ($t = \text{sim}(\mathbf{x}, \mathbf{x}^-) - \text{sim}(\mathbf{x}, \mathbf{x}^+)$) is zero, a fixed penalty of $\log 2$ is enforced as the representation is not discriminative on intra-variance. Definition of \mathbf{x}^+ and \mathbf{x}^- is in section 4.2. As θ becomes larger, derivative at $t = 0$ keeps increasing and the penalty quickly increases when the ranking measure is wrong ($t > 0$) and decreases when it is correct. Besides, when the ranking is correct, penalties enforced are close to zero as long as t is smaller than a margin value that is monotonically increasing with θ . As shown in Figure 3 (b), as θ decreases from 1.0 to 0.01, model performance keeps increasing, validating our hypothesis that a small enough margin is more beneficial. However, when θ is too small as 0.001, l_{rank} is too sensitive at $t = 0$, leading to unstable training. One thing need to mention here is that we use 0.05 as the θ value in other experiments and performance comparison, which is not optimal. $\theta = 0.01$ can further increase accuracy on UCF101 and HMDB51 by 0.19% and 1.71% respectively.

Performance comparison We compare our method with previous works on both downstream supervised finetuning task and video retrieval task. As shown in the figure, we classify previous methods into 3 categories according to whether they are pretext-task based, contrastive learning based or hybrid of the two. We do not compare to recent methods [6, 22, 27] as they either use much larger backbone and input size or use optical flow. We outperform methods based on two mainstream pretext tasks: temporal order [16, 20, 38] and pace [23, 24, 33]. SpeedNet [23] and TempTrans [24] achieved superior performance only when the input size or backbone is advantageous. MemDPC [9] predicted future states and applies spatial-temporal contrastive loss on features. It however also relies on huge input size. Our model achieves higher performance than MoCo based method BE [34] and VideoMoCo [28]. RSPNet[21] is the state-of-the-art method improving upon Pace [33] by predicting relative speedness. Our model surpasses RSPNet by 0.9% and 6.6% on UCF101 and HMDB51 test

Table 3: Finetuning performance comparison.

Method	Input Size	Arch	#param.	pretrain	UCF101	HMDB51
Pretext Task						
Shuffle&Learn[20]	$3 \times 256 \times 256$	AlexNet	58.3M	UCF101	50.2	18.1
OPN[16]	$4 \times 80 \times 80$	VGG	8.6M	UCF101	59.8	23.8
VCP[19]	$16 \times 112 \times 112$	R(2+1)D	14.4M	UCF101	66.3	32.2
VCOP[38]	$16 \times 112 \times 112$	R(2+1)D	14.4M	UCF101	72.4	30.9
PRP[39]	$16 \times 112 \times 112$	R(2+1)D	14.4M	UCF101	72.1	35.0
SpeedNet[23]	$64 \times 224 \times 224$	S3D-G	9.6M	K400	81.1	48.8
TempTrans[24]	$16 \times 112 \times 112$	R(2+1)D-18	33.2M	UCF101	81.6	46.4
Contrastive						
MemDPC[9]	$40 \times 224 \times 224$	3D-ResNet34	32.4M	K400	78.1	41.2
VideoMoCo[28]	$32 \times 112 \times 112$	R(2+1)D	14.4M	K400	78.7	49.2
BE(MoCo)[34]	$16 \times 112 \times 112$	C3D	27.7M	UCF101	72.4	42.3
IIC[26]	$16 \times 112 \times 112$	R3D	14.4M	UCF101	74.4	38.3
Hybrid						
Pace[33]	$16 \times 112 \times 112$	R(2+1)D	14.4M	K400	77.1	36.6
RSPNet[21]	$16 \times 112 \times 112$	R(2+1)D	14.4M	K400	81.1	44.6
Ours(MoCo)	$16 \times 112 \times 112$	R(2+1)D	14.4M	UCF101	78.5	47.5
Ours(SimCLR)	$16 \times 112 \times 112$	R(2+1)D	14.4M	UCF101	79.0	45.4
Ours(SimCLR)	$16 \times 112 \times 112$	R(2+1)D	14.4M	K400	82.0	51.2

Table 4: Video retrieval performance comparison.

	Arch	Top-k				
		k=1	k=5	k=10	k=20	k=50
PRP[39]	C3D	23.2	38.1	46.0	55.7	68.4
Pace[33]	R(2+1)D	25.6	42.7	51.3	61.3	74.0
TempTrans[24]	3D-ResNet18	26.1	48.5	59.1	69.6	82.8
RSPNet[21]	3D-ResNet18	41.1	59.4	68.4	77.8	88.7
Ours	R(2+1)D	46.7	63.1	69.7	78.0	87.8

set. Even pretrained on the much smaller UCF101 training data, our model still exhibits excellent performance with 0.8% higher HMDB51 accuracy upon kinetics-400 pretrained RSPNet.

On video retrieval task, our method still exhibit robust performance. Our top-1 retrieval accuracy reaches 46.7%, improving upon RSPNet by 5.6%. This shows our model has a well learned discrimination ability.

6 Conclusion

In this paper, we approach self-supervised video representation learning from the perspective of inter-intra variance. We find that existing contrastive learning solution can not learn good embedded features that genuinely encode intra-variance in videos. Therefore, we propose to learn dual representations which encodes both inter-variance and intra-variance by a shuffle-rank pretext task and a temporal coherent contrastive loss. It also surpasses both pretext-task based and contrastive learning based counterparts on classification and video retrieval tasks on UCF101 and HMDB51 dataset. However, as self-supervised video recognition is a resource-exhaustive task, we cannot provide more experiment results on very large backbones and large-scale dataset. To facilitate future research and for a better comparison, we provide our code and implementation details in supplementary material. On the negative side of this research, as unlabeled data becoming more beneficial, the behavior of using unlabeled data for pretraining should develop under reasonable regularization otherwise would

infringe people’s privacy. We therefore suggest to regularize the phenomenon of making use of self-supervised learning for commercial usage.

References

- [1] Y. Bai, F. Gao, Y. Lou, S. Wang, T. Huang, and L.-Y. Duan. Incorporating intra-class variance to fine-grained visual recognition. In *ICME*, 2018.
- [2] C. Burges, T. Shaked, E. Renshaw, A. Lazier, M. Deeds, N. Hamilton, and G. Hullender. Learning to rank using gradient descent. In *ICML*, 2005.
- [3] M. Caron, I. Misra, J. Mairal, P. Goyal, P. Bojanowski, and A. Joulin. Unsupervised learning of visual features by contrasting cluster assignments. In *NeurIPS*, 2020.
- [4] T. Chen, S. Kornblith, M. Norouzi, and G. Hinton. A simple framework for contrastive learning of visual representations. In *ICML*, 2020.
- [5] W. Chen, T.-y. Liu, Y. Lan, Z.-m. Ma, and H. Li. Ranking measures and loss functions in learning to rank. In *NeurIPS*, 2009.
- [6] C. Feichtenhofer, H. Fan, B. Xiong, R. Girshick, and K. He. A large-scale study on unsupervised spatiotemporal representation learning. In *CVPR*, 2021.
- [7] B. Fernando, H. Bilen, E. Gavves, and S. Gould. Self-supervised video representation learning with odd-one-out networks. In *CVPR*, 2017.
- [8] J.-B. Grill, F. Strub, F. Altché, C. Tallec, P. H. Richemond, E. Buchatskaya, C. Doersch, B. A. Pires, Z. D. Guo, M. G. Azar, B. Piot, K. Kavukcuoglu, R. Munos, and M. Valko. Bootstrap your own latent: A new approach to self-supervised learning. *arxiv:2006.07733*, 2020.
- [9] T. Han, W. Xie, and A. Zisserman. Memory-augmented dense predictive coding for video representation learning. In *ECCV*, 2020.
- [10] K. He, H. Fan, Y. Wu, S. Xie, and R. Girshick. Momentum contrast for unsupervised visual representation learning. In *CVPR*, 2020.
- [11] W. Kay, J. Carreira, K. Simonyan, B. Zhang, C. Hillier, S. Vijayanarasimhan, F. Viola, T. Green, T. Back, P. Natsev, M. Suleyman, and A. Zisserman. The kinetics human action video dataset. *arXiv:1705.06950*, 2017.
- [12] D. Kim, D. Cho, and I. S. Kweon. Self-supervised video representation learning with space-time cubic puzzles. In *AAAI*, 2018.
- [13] T. Kobayashi. Large margin in softmax cross-entropy loss. In *BMVC*, 2019.
- [14] Q. Kong, W. Wei, Z. Deng, T. Yoshinaga, and T. Murakami. Cycle-contrast for self-supervised video representation learning. In *NeurIPS*, 2020.
- [15] H. Kuehne, H. Jhuang, E. Garrote, T. Poggio, and T. Serre. HMDB: a large video database for human motion recognition. In *ICCV*, 2011.
- [16] H.-Y. Lee, J.-B. Huang, M. K. Singh, and M.-H. Yang. Unsupervised representation learning by sorting sequence. In *ICCV*, 2017.
- [17] B. Liu, Y. Cao, Y. Lin, Q. Li, Z. Zhang, M. Long, and H. Hu. Negative margin matters: Understanding margin in few-shot classification. In *ECCV*, 2020.
- [18] J. Liu, Y. Sun, C. Han, Z. Dou, and W. Li. Deep representation learning on long-tailed data: A learnable embedding augmentation perspective. In *CVPR*, 2020.
- [19] D. Luo, C. Liu, Y. Zhou, D. Yang, C. Ma, Q. Ye, and W. Wang. Video cloze procedure for self-supervised spatio-temporal learning. In *AAAI*, 2020.
- [20] I. Misra, C. L. Zitnick, and M. Hebert. Shuffle and learn: Unsupervised learning using temporal order verification. In *ECCV*, 2016.
- [21] C. Peihao, H. Deng, H. Dongliang, L. Xiang, Z. Runhao, W. Shilei, T. Mingkui, and G. Chuang. Rspnet: Relative speed perception for unsupervised video representation learning. In *AAAI*, 2021.
- [22] Q. Rui, M. Tianjian, G. Boqing, Y. Ming-Hsuan, W. Huisheng, B. Serge, and C. Yin. Spatiotemporal contrastive video representation learning. In *CVPR*, 2021.
- [23] B. Sagie, E. Ariel, L. Oran, M. Inbar, W. T. Freeman, R. Michael, I. Michal, and D. Tali. Speednet: Learning the speediness in videos. In *CVPR*, 2020.
- [24] J. Simon, M. Givi, and F. Paolo. Video representation learning by recognizing temporal transformations. In *ECCV*, 2020.

- [25] K. Soomro, A. R. Zamir, and M. Shah. Ucf101: A dataset of 101 human actions classes from videos in the wild. *arxiv:1212.0402*, 2012.
- [26] L. Tao, X. Wang, and T. Yamasaki. Self-supervised video representation learning using inter-intra contrastive framework. In *ACMMM*, 2020.
- [27] H. Tengda, X. Weidi, and Z. Andrew. Coclr: Self-supervised co-training for video representation learning. In *NeurIPS*, 2020.
- [28] P. Tian, S. Yibing, Y. Tianyu, J. Wenhao, and L. Wei. Videomoco: Contrastive video representation learning with temporally adversarial examples. In *CVPR*, 2021.
- [29] W. Tongzhou and I. Phillip. Understanding contrastive representation learning through alignment and uniformity on the hypersphere. In *ICML*, 2020.
- [30] D. Tran, H. Wang, L. Torresani, J. Ray, Y. LeCun, and M. Paluri. A closer look at spatiotemporal convolutions for action recognition. In *CVPR*, 2018.
- [31] A. van den Oord, Y. Li, and O. Vinyals. Representation learning with contrastive predictive coding. *arXiv:1807.03748*, 2019.
- [32] J. Wang, J. Jiao, L. Bao, S. He, Y. Liu, and W. Liu. Self-supervised spatio-temporal representation learning for videos by predicting motion and appearance statistics. In *CVPR*, 2019.
- [33] J. Wang, J. Jiao, and Y. Liu. Self-supervised video representation learning by pace prediction. In *ECCV*, 2020.
- [34] J. Wang, Y. Gao, K. Li, Y. Lin, A. J. Ma, H. Cheng, P. Peng, R. Ji, and X. Sun. Removing the background by adding the background: Towards background robust self-supervised video representation learning. In *CVPR*, 2021.
- [35] D. Wei, J. J. Lim, A. Zisserman, and W. T. Freeman. Learning and using the arrow of time. In *CVPR*, 2018.
- [36] Z. Wu, Y. Xiong, X. Y. Stella, and D. Lin. Unsupervised feature learning via non-parametric instance discrimination. In *CVPR*, 2018.
- [37] S. Xie, C. Sun, J. Huang, Z. Tu, and K. Murphy. Rethinking spatiotemporal feature learning: Speed-accuracy trade-offs in video classification. In *ECCV*, 2018.
- [38] D. Xu, J. Xiao, Z. Zhao, J. Shao, D. Xie, and Y. Zhuang. Self-supervised spatiotemporal learning via video clip order prediction. In *CVPR*, 2019.
- [39] Y. Yao, C. Liu, D. Luo, Y. Zhou, and Q. Ye. Video playback rate perception for self-supervised spatiotemporal representation learning. In *CVPR*, 2020.

Appendix

A Implementation details

Self-supervised pretrain In self-supervised pretraining stage, we resize each frame to 128×171 and randomly crop images to size of 112×112 in a temporal consistent way. Each input clip has 16 frames with temporal interval of 4. Data augmentations include random color jittering, horizontal flipping and gaussian blurring. We pretrain the model for 200 epochs with an SGD optimizer with an initial learning rate of 0.003, weight decay of $1e-4$ and momentum of 0.9. Learning rate is divided by 10 at epoch 120 and 160. Batch size is set to 64. We pretrain the model on 8 Tesla V100 GPUs. Pretrained weights at epoch 190 is selected for evaluation. Size of the MoCo negative queue is set to 16,384. We pretrain on UCF101 training split in all ablation studies and provide pretraining result on large-scale Kinetics400 for performance comparison with previous works. We set $\tau, \tau_{tc}, \theta, \lambda_1, \lambda_2$ to 0.07, 0.5, 0.05, 1.0 and 1.0, respectively.

Supervised finetuning During supervised finetuning, we replace the nonlinear projection head in pretraining stage with a one-layer classification layer. The backbone is initialized with the pretrained weights while the classification head is randomly initialized. Similar as pretraining stage, each clip contains 16 frames sampled at a pace equals to 2. Each frame is first resized to 128×171 and then randomly cropped to size of 112×112 in a temporal consistent way. Data augmentations include color jittering and horizontal flipping. We finetune all layers for 150 epochs using a SGD optimizer with momentum of 0.9. Learning rate is set to 0.05 and divided by 10 at epoch 50 and 100. Batchsize is set to 64.

Finetuning testing After finetuning, we test classification accuracy on the test splits. 10 16-frame clips are temporarily and uniformly sampled in each video with a pace equals to 2. No data augmentation is applied. Each frame is first resized to 128×171 and then center cropped to size of 112×112 . Classification probabilities are averaged among the 10 clips for each video.

Video retrieval We compute average features of 10 clips uniformly sampled from each video using the pretrained backbone. Setting is the same as the *Finetuning testing* stage except that we use a pace equals to 4 to be consistent with the pretraining stage. Feature vectors are computed through spatial-temporal average pooling the last layer output of the backbone and then normalized. Cosine similarity is adopted. We conduct video retrieval on UCF101 to retrieve test videos using training videos and calculate the top- k accuracy ($k = 1, 5, 10, 20, 50$).

B Comparison with shuffling order prediction

Table 5: Comparison between order prediction (OP) and our proposed shuffle-rank (SR). Models are pretrained on UCF101 training set.

	UCF101	HMDB51
SimCLR+OP	75.39	32.38
SimCLR+SR	76.82	40.05

C Backbone architecture

We provide architectures of R3D and R(2+1)D in Table 6. As the structure of S3D-G is too complicated to be put in a table, we ask the reader to refer to [37] for more details. We use the same implementation in our code.

D Measure inter and intra variances

We provide our mathematical formulations of inter-variance and intra-variance for calculating inter and intra variances. Formally, let μ_k represent the mean embedded feature of the k -th video. We use S_k to represent the hierarchical relation between clips $\{c_i\}_{i=1}^M$ and videos $\{V_i\}_{i=1}^N$, i.e. $S_k = \{i|c_i \in V_k\}$. We define intra-variance as the average variances within clip features sampled from the same video, and inter-variance as the average

Table 6: architecture of R3D and R(2+1)D we used in experiments.

layer name	output size	R3D	R(2+1)D
conv1	$L \times 56 \times 56$	$3 \times 3 \times 3, 64$, stride $1 \times 2 \times 2$	
conv2_x	$L \times 56 \times 56$	$\begin{bmatrix} 3 \times 3 \times 3, 64 \\ 3 \times 3 \times 3, 64 \end{bmatrix} \times 1$	$\begin{bmatrix} 1 \times 3 \times 3, 64 \\ 3 \times 1 \times 1, 64 \end{bmatrix} \times 2$
conv3_x	$\frac{L}{2} \times 28 \times 28$	$\begin{bmatrix} 3 \times 3 \times 3, 128 \\ 3 \times 3 \times 3, 128 \end{bmatrix} \times 1$	$\begin{bmatrix} 1 \times 3 \times 3, 128 \\ 3 \times 1 \times 1, 128 \end{bmatrix} \times 2$
conv4_x	$\frac{L}{4} \times 14 \times 14$	$\begin{bmatrix} 3 \times 3 \times 3, 256 \\ 3 \times 3 \times 3, 256 \end{bmatrix} \times 1$	$\begin{bmatrix} 1 \times 3 \times 3, 256 \\ 3 \times 1 \times 1, 256 \end{bmatrix} \times 2$
conv5_x	$\frac{L}{8} \times 7 \times 7$	$\begin{bmatrix} 3 \times 3 \times 3, 512 \\ 3 \times 3 \times 3, 512 \end{bmatrix} \times 1$	$\begin{bmatrix} 1 \times 3 \times 3, 512 \\ 3 \times 1 \times 1, 512 \end{bmatrix} \times 2$
	$1 \times 1 \times 1$	spatial-temporal global average pooling	

pairwise distance between videos:

$$\mu_k = \frac{1}{S_k} \sum_{i \in S_k} \mathbf{z}_i \quad (4)$$

$$\sigma_{intra} = \frac{1}{N} \sum_{k=1}^N \frac{1}{|S_k|} \sum_{i \in S_k} \|\mathbf{z}_i - \mu_k\|_2^2 \quad (5)$$

$$\sigma_{inter} = \frac{1}{N(N-1)} \sum_{i=1}^{N-1} \sum_{j=i+1}^N \|\mu_i - \mu_j\|_2^2 \quad (6)$$

where \mathbf{z} is the encoded feature vector as introduced in the paper. This formulation is adapted from Liu et al. [17].

E Effect of contrastive loss on inter and intra variance

We provide theoretical analysis to our statement in preliminary section that contrastive loss suppresses the learning of σ_{inter} and encourages learning σ_{intra} . Our analysis follows discussion of Tongzhou and Phillip [29]. Following our definition in preliminary section, clip contrastive loss can be written in the form of

$\mathcal{L}_c = -\frac{1}{M} \sum_{i=1}^M \log \frac{\exp(\frac{\mathbf{z}_i \cdot \mathbf{z}_{i^+}}{\tau})}{\sum_{k=1}^M \mathbf{1}_{[k \neq i]} \exp(\frac{\mathbf{z}_i \cdot \mathbf{z}_k}{\tau})}$, which can be transformed into:

$$\mathcal{L}_c = -\frac{1}{M} \sum_{i=1}^M \frac{\mathbf{z}_i \cdot \mathbf{z}_{i^+}}{\tau} + \frac{1}{M} \sum_{i=1}^M \left[\log \left(\exp\left(\frac{\mathbf{z}_i \cdot \mathbf{z}_{i^+}}{\tau}\right) + \sum_{k=1, k \notin \{i, i^+\}}^M \exp\left(\frac{\mathbf{z}_i \cdot \mathbf{z}_k}{\tau}\right) \right) \right] \quad (7)$$

where M is the number of sampled clips, \mathbf{z} is normalized encoded clip feature vector and τ is the temperature parameter. As explained in [29], since $\sum_{k=1, k \notin \{i, i^+\}}^M \exp(\mathbf{z}_i \cdot \mathbf{z}_k / \tau)$ is always positive and bounded below, the loss favors smaller $-\frac{1}{M} \sum_{i=1}^M \mathbf{z}_i \cdot \mathbf{z}_{i^+} / \tau$, which is equivalent to decreasing σ_{intra} as the sample size M goes to infinity. On the other hand, when fixing σ_{intra} , minimizing the loss is equivalent to decreasing

$$\frac{1}{M} \sum_{i=1}^M \left[\log \left(t_i + \sum_{k=1, k \notin \{i, i^+\}}^M \exp(\mathbf{z}_i \cdot \mathbf{z}_k / \tau) \right) \right] \quad (8)$$

where $t_i = \exp(\mathbf{z}_i \cdot \mathbf{z}_{i^+} / \tau)$ is a random variable when σ_{intra} is fixed. Hence, equation 8 measures similarity between features from different instances. Minimizing equation 8 is thus equivalent to minimizing inter-variance σ_{inter} . Therefore, contrastive loss encourages decreasing intra-variance and increasing inter-variance.

F Training algorithm

F.1 Training SimCLR

Algorithm 1: Training SimCLR

Input: batch size N , backbone f , clip projector f_c , dual projector f_r , videos V ;

while *training not converge* **do**

 sample minibatch $\{v_i\}_{i=1}^N$ from V ;

for *all* $i \in \{1, 2, \dots, N\}$ **do**

 sample and augment two clips c_i^1 and c_i^2 from v_i ;

$\mathbf{h}_i^1 = f(c_i^1)$;

$\mathbf{h}_i^2 = f(c_i^2)$;

 /* clip projection */

$\mathbf{z}_{2i-1} = f_c(\mathbf{h}_i^1)$;

$\mathbf{z}_{2i} = f_c(\mathbf{h}_i^2)$;

 /* dual projection */

$\mathbf{r}_{2i-1} = f_r(\mathbf{h}_i^1)$;

$\mathbf{r}_{2i} = f_r(\mathbf{h}_i^2)$;

 /* shuffling and dual projection */

 augment c_i^1 into s_i and randomly shuffle s_i into \hat{s}_i ;

$\mathbf{q}_i = f_r(f(s_i))$;

$\mathbf{p}_i = f_r(f(\hat{s}_i))$;

end

 calculate \mathcal{L}_c on $\{\mathbf{z}\}_{i=1}^{2N}$;

 calculate \mathcal{L}_{tc} on $\{\mathbf{r}\}_{i=1}^{2N}$;

 calculate $\mathcal{L}_{rank}^{unaug}$ on $\{\mathbf{r}_{2i-1}, \mathbf{p}_i\}_{i=1}^N$ and \mathcal{L}_{rank}^{aug} on $\{\mathbf{q}_i, \mathbf{p}_i\}_{i=1}^N$;

 update f , f_c and f_r using stochastic gradient descent;

end

F.2 Training MoCo

Unlike SimCLR, negative examples in MoCo come from the dictionary $\{\mathbf{k}_i\}_{i=1}^m$ while positive example is the sampled augmented clip \mathbf{k}^+ . m is set to 16384. So contrastive loss is denoted as :

$$\mathcal{L}_c = -\frac{1}{N} \sum_{i=1}^N \frac{\exp(\mathbf{z}_i \cdot \mathbf{k}_i^+ / \tau)}{\exp(\mathbf{z}_i \cdot \mathbf{k}_i^+ / \tau) + \sum_{j=1}^m \exp(\mathbf{z}_i \cdot \mathbf{k}_j / \tau)} \quad (9)$$

As for temporal coherent contrast, an extra dictionary for dual representations $\{\mathbf{d}_i\}_{i=1}^m$ is maintained. Dual representations are denoted as \mathbf{r} instead of \mathbf{z} . Replacing dot product similarity, dictionary \mathbf{k} , projected feature \mathbf{z} with tc-sim, \mathbf{d} and \mathbf{r} in equation 9 leads us to MoCo's temporal coherent contrast loss:

$$\mathcal{L}_{tc} = -\frac{1}{N} \sum_{i=1}^N \frac{\exp(\text{tc-sim}(\mathbf{r}_i, \mathbf{d}_i^+) / \tau)}{\exp(\text{tc-sim}(\mathbf{r}_i, \mathbf{d}_i^+) / \tau) + \sum_{j=1}^m \exp(\text{tc-sim}(\mathbf{r}_i, \mathbf{d}_j) / \tau)} \quad (10)$$

We provide training algorithm on MoCo here.

Algorithm 2: Training MoCo

Input: batch size N , backbone $f_q f_k$, clip projectors $g_q g_k$, dual projectors $h_q h_k$, videos V , clip feature dictionary $\{\mathbf{k}_i\}_{i=1}^m$ and dual feature dictionary $\{\mathbf{d}_i\}_{i=1}^m$;

while *training not converge* **do**

sample minibatch $\{v_k\}_{k=1}^N$ from V ;

for all $i \in \{1, 2, \dots, N\}$ **do**

sample and augment two clips c_i^1 and c_i^2 from v_i , c_i^2 is treated as positive pair of c_i^1 ;

$\mathbf{b}_i^1 = f_q(c_i^1)$;

$\mathbf{b}_i^2 = f_k(c_i^2)$;

/* clip projection */

$\mathbf{z}_i = g_q(\mathbf{b}_i^1)$;

$\mathbf{k}_i^+ = g_k(\mathbf{b}_i^2)$;

$\mathbf{k}_i^+ = \mathbf{k}_i^+.detach()$; // stop gradient

/* dual projection */

$\mathbf{r}_i = h_q(\mathbf{b}_i^1)$;

$\mathbf{d}_i^+ = h_k(\mathbf{b}_i^2)$;

$\mathbf{d}_i^+ = \mathbf{d}_i^+.detach()$; // stop gradient

/* shuffling and dual projection */

augment c_i^1 into s_i and randomly shuffle s_i into \hat{s}_i ;

$\mathbf{q}_i = h_q(f_q(s_i))$;

$\mathbf{p}_i = h_q(f_q(\hat{s}_i))$;

end

calculate \mathcal{L}_c on positive pairs $\{\mathbf{z}_i, \mathbf{k}_i^+\}_{i=1}^N$ and negative queue $\{\mathbf{k}_i\}_{i=1}^m$;

calculate \mathcal{L}_{tc} on positive pairs $\{\mathbf{r}_i, \mathbf{d}_i^+\}_{i=1}^N$ and negative queue $\{\mathbf{d}_i\}_{i=1}^m$;

calculate $\mathcal{L}_{rank}^{unaug}$ on $\{\mathbf{r}_i, \mathbf{p}_i\}_{i=1}^N$ and \mathcal{L}_{rank}^{aug} on $\{\mathbf{q}_i, \mathbf{p}_i\}_{i=1}^N$;

momentum update f_k, g_k and h_k by f_q, g_q and h_q respectively;

update f_q, g_q and h_q using stochastic gradient descent;

$enqueue(\{\mathbf{k}_i\}_{i=1}^m, \{\mathbf{k}_i^+\}_{i=1}^N)$;

$dequeue(\{\mathbf{k}_i\}_{i=1}^m)$;

$enqueue(\{\mathbf{d}_i\}_{i=1}^m, \{\mathbf{d}_i^+\}_{i=1}^N)$;

$dequeue(\{\mathbf{d}_i\}_{i=1}^m)$;

end

G Feature distribution comparison

We visualize the feature distribution encoded by baseline SimCLR and our pretrained models on UCF101 test set. As shown, feature distribution of baseline SimCLR is very sparse, with large margin between different classes. With our shuffle-rank pretext task, intra-variance becomes larger, resulting in a denser distribution. Further equipping the model with temporal coherent contrastive loss makes the clustering borders clearer. This is consistent with our inter-intra variance motivation.

H Attention visualization

To qualitatively measure the learned features, we draw heatmaps output from last layer of pretrained models. Specifically, we apply average pooling on last layer feature maps along both feature channel and temporal channel, i.e. from a size of (C, T, H, W) into (H, W) , to obtain a heatmap. Such heatmap is then added to each frame of the input clip for visualization. As shown in Figure 5, baseline SimCLR can be easily distracted by surrounding backgrounds, while our proposed method always focus on areas with motion semantics.

I Video retrieval visualization

In Figure 6, we visualize the video retrieval result of the integrated pretrained model (SimCLR+SR+TC). We pretrain the model on Kinetics-400 and conduct retrieval experiment on UCF101. It can be observed that our

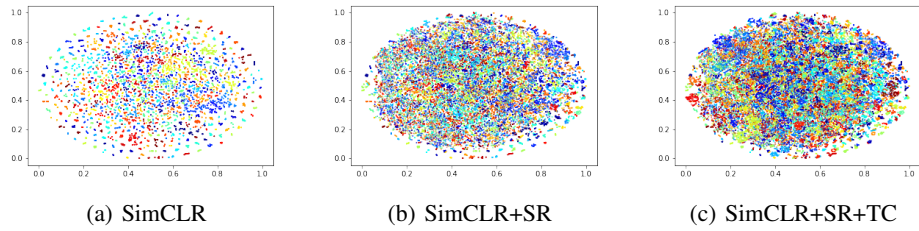


Figure 4: t-SNE visualization of features encoded by pretrained models. Models are pretrained on UCF101 train split and features are computed on UCF101 test split.

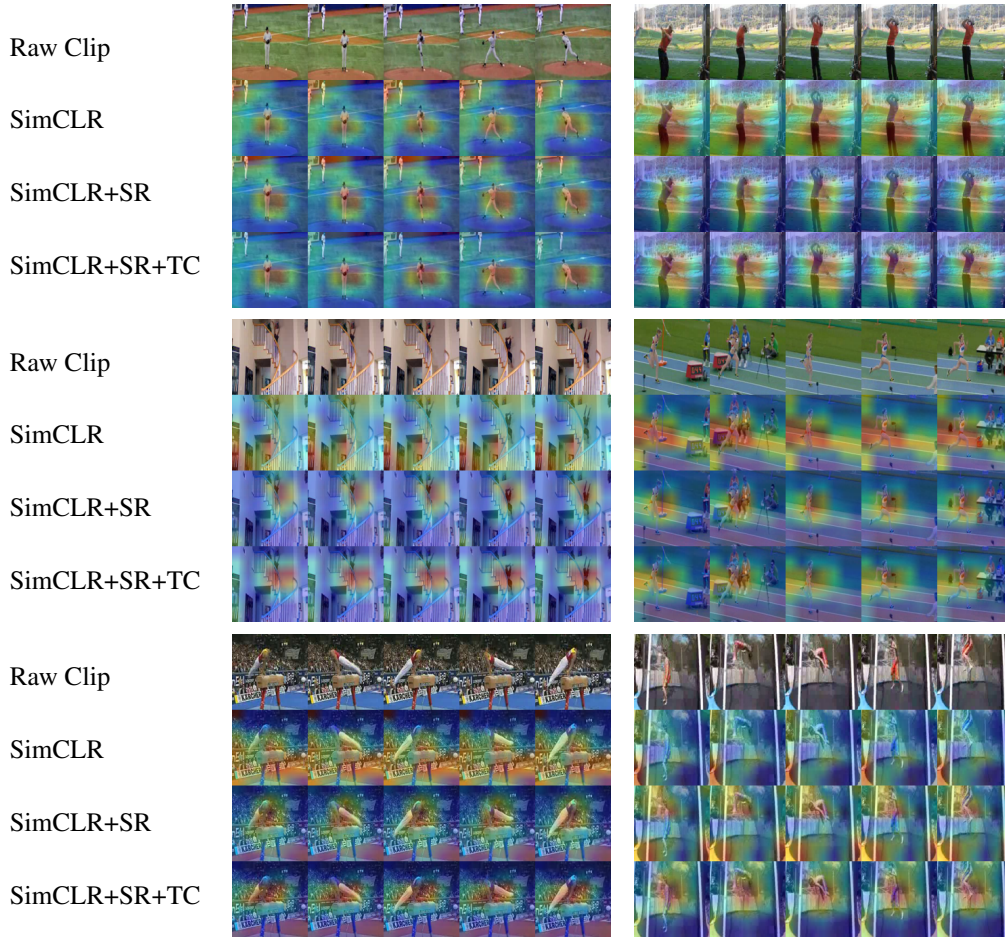


Figure 5: Heatmap visualization. The warmer the color is, the larger the response is. Zoom in for visualization.

retrieval results are not perfect in that videos from different categories can be retrieved if having similar actions and contents, e.g. image 3 (ApplyLipstick) of ApplyEyeMakeup, image 3 (Shotput) of GolfSwing, image 3 (ParallelBars) of BalanceBeam and image 3 (BalanceBeam) of ParallelBars.

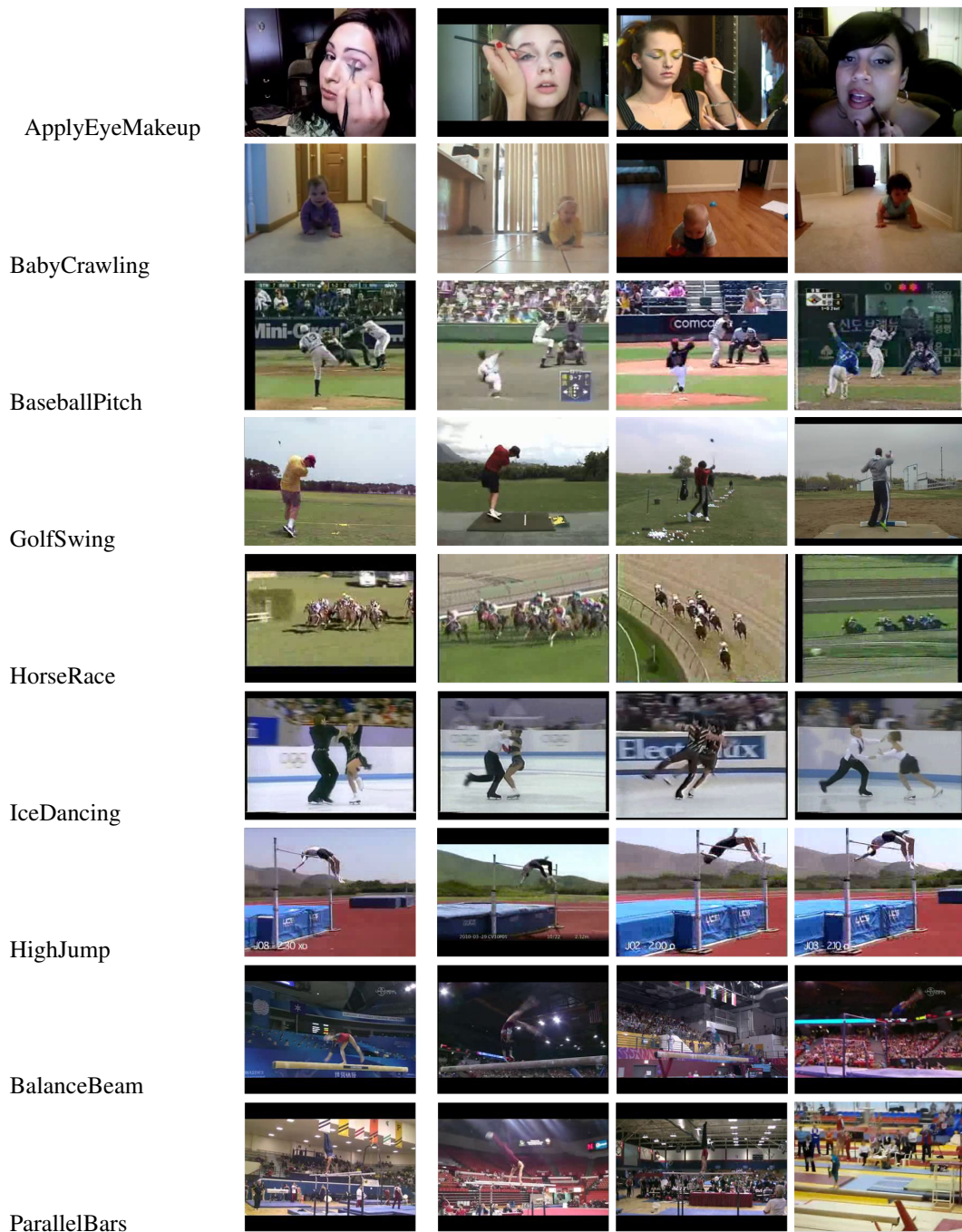


Figure 6: Video retrieval visualization. The first and second column are categories and images of test instance, respectively. The rightmost 3 columns are nearest retrieval results. We select an image from the video for demonstration.